ARTICLE OPEN

Check for updates

Influence of radiation on borosilicate glass leaching behaviors

Kemian Qin[1,2,3], Buyun Zhang[1,2,3], Zhaoxuan Jin[1,2,3], Yuchuan Wang[2], Yuhe Pan[1,2,3], Yuqian Sun[1,2,3], Kai Bai[1,2,3], Shikun Zhu[1,2,3], Tieshan Wang[1,2,3] and Haibo Peng[1,2,3]✉

Vitrification is widely recognized as a promising method for the geological disposal of high-level radioactive waste (HLW) worldwide. To ensure the safe disposal of radioactive waste, the borosilicate glass that vitrifies HLW must exhibit exceptional water resistance to prevent the possibility of groundwater corrosion and subsequent radioactive leaks. Radiation might change the water resistance of borosilicate glass. A series of zirconium-containing borosilicate glass with an irradiation dose of 0.3 dpa were utilized to examine the radiation effect on glass-water interaction. Scanning electron microscopy (SEM), Time-of-Flight Secondary ion mass spectrometry (ToF-SIMS), X-ray photoelectron spectroscopy (XPS), Inductively Coupled Plasma Optical Emission spectroscopy (ICP-OES) and Fourier transform infrared spectroscopy (FTIR) were used to investigate the leaching behavior of the non- and irradiated samples. The depth profile of the leached samples implied the interdiffusion dominated glass-water interaction. The results from FTIR and ICP-OES indicated that, after irradiation, the initial leaching rate increased by threefold. Additionally, the impact of different zirconium contents on the water resistance of borosilicate glass was also presented.

npj Materials Degradation (2024)8:9 ; https://doi.org/10.1038/s41529-024-00426-0

INTRODUCTION

Borosilicate glass is a widely used material in the nuclear industry for immobilizing high-level radioactive waste (HLW)[1–4]. The safety and stability of the vitrification over the long-term disposal are dependent on the retention of radionuclides within the glass matrix[4–10]. Numerous previous studies have investigated the macroscopic and microscopic changes that occur in borosilicate glasses after irradiation[11–21]. It has been found that the internal irradiation causes the degeneration in both glass mechanical properties and leaching resistance during the long-term disposal[22,23]. Therefore, understanding the radiation effect and leaching behavior of borosilicate glass is critical for evaluating the long-term performance of the waste form and ensuring the safety of nuclear waste repositories.

Previous research has extensively studied the leaching behavior and mechanism of borosilicate glass[3,24–27]. According to existing literature, the dissolution process of this type of glass can be generally divided into three stages based on the different leaching rates observed: the initial stage, the residual stage, and the third stage which exists different situations[28,29]. During the initial stage of the interaction between glass and water, the diffusion of H^+ ions from water can replace alkali metal ions in the glass network. This phenomenon leads to the loss of network-modifying ions, whose concentration in the solution is typically dependent on the square-root of leaching time[24]. In addition, results have suggested that such diffusion effects may not be limited solely to glass network modifiers. Gin et al.[30] observed that even at silica-saturated leachate, the boron release rate from borosilicate glass still followed a square root time dependence. They suggested that the loss of sodium ions altered the glass structure, particularly the boron-related structures[31]. Loss of a sodium ion from a BO tetrahedron ($[BO_4]$) leads to the conversion of boron from coordination number IV to III ($[BO_3]$), facilitating the diffusion of boron. Gin et al.[32] also studied leaching behavior of the aluminoborosilicate glass after swift heavy ion irradiation. Mougnaud et al.[33] conducted a study on the change in leaching rate of borosilicate glass after external irradiation and found that the thickness of alteration also followed the diffusion law. Peuget et al.[34] compared the effect of internal decay and heavy ion irradiation on leaching behavior, suggested that the effect of ion irradiation was overestimated due to the absence of alpha decay. Tribet et al.[35] investigated the leaching behavior of International Simple Glass (ISG) after Au radiation and pointed out that radiation can increase the reactivity of water in the alteration-layer/glass interface. Mir et al.[23] reported the microstructural change of vitrification after 21 years of water corrosion and studied the re-healing porous alter layer of borosilicate glass after irradiation. Zhang et al.[36] found that with ion irradiation, $[BO_4]$ units will transmitted to $[BO_3]$ units for ternary borosilicate glass, and the leaching rate increased significantly. Improving our understanding of the mechanisms and factors that control the leaching behavior of borosilicate glass is critical for developing accurate models to predict the long-term performance of the waste form. This can inform the design and assessment of nuclear waste repositories and ensure the safe and effective disposal of high-level radioactive waste. Continued research into the leaching behavior of borosilicate glass is therefore essential for advancing our understanding of nuclear waste management and reducing the potential risks to the environment and human health.

In this work, the leaching behavior of sodium borosilicate glass with varying concentrations of zirconia doping after ion irradiation was investigated. SEM/EDS and XPS were used to explore the element distribution on the surface and the cross-section of the glass after leaching. ToF-SIMS was employed to give the depth profile of sample after leaching. The element loss during water-glass reactions was measured using inductively coupled plasma optical emission spectrometry (ICP-OES), while the surface structure of the glass was analyzed through in-situ Fourier transform infrared (FTIR) spectra. The results demonstrated the usefulness of FTIR in providing insights into the effects of radiation on leaching behavior, which is consistent with the results obtained by ICP-OES. The relationship between the structural changes and

[1]MOE Frontiers Science Center for Rare Isotopes, Lanzhou University, Lanzhou, China. [2]School of Nuclear Science and Technology, Lanzhou University, Lanzhou, China. [3]Key Laboratory of Special Function Materials and Structure Design Ministry of Education, Lanzhou University, Lanzhou, China. ✉email: penghb@lzu.edu.cn

element loss was also examined. In addition, the in-situ FTIR analysis revealed the impact of glass components on the water-glass interaction, which was not apparent from the ICP-OES results.

RESULTS

Irradiation effect

The change of surface structure of ZNBS series after Xe ion irradiation were examined via ATR-FTIR, as shown in Fig. 1. The ATR-FTIR spectrum of ZNBS series glass were normalized at their maximum value to compare the change of surface structure. The FTIR spectra of ZNBS series exhibit several characteristic peaks, including the stretching vibration mode of the B-O-B unit[21,37] at around 700 cm^{-1}, and the stretching vibration mode of the O-Si-O unit[38] at around 780 cm^{-1}. Other notable peaks include the stretching vibration of the B-O-Si bond[39] at 945 cm^{-1}, the stretching vibration of the Si–O–Si bond in the Q^3structural unit[39] at 1050 cm^{-1}, and the stretching vibration of the Si-O-Si bond in the Q^4 structural unit[39] at 1150 cm^{-1}. The stretching vibration of the B–O bond in the [BO_3] structural unit[36] is observed at around 1250–1550 cm^{-1}.

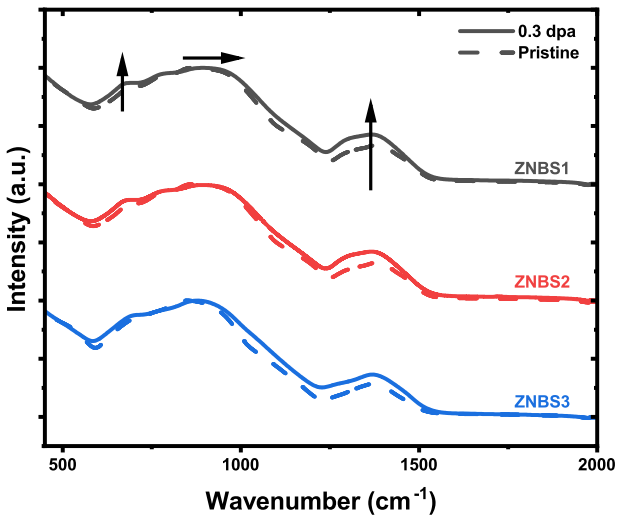

Fig. 1 Normalized ATR-FTIR spectra for ZNBS series before and after ion irradiation. The dashed lines refer to the FTIR spectra of pristine ZNBS series glass, and the soild lines for irradiated samples.

There are three noticeable changes in Fig. 1: (a) the intensity increasing at around 700 cm^{-1}; (b) the peak shift from around 850 to 900 cm^{-1}; and (c) the surge of the intensity for [BO_3]-related region. Since the thickness of radiation layer is less than 2 μm form SRIM simulation, the irradiation-induced change in [BO_3] unit ranging from 1250 to 1500 cm^{-1} can be properly investigated by ATR-FTIR. After irradiation, the area of [BO_3] increased 15%, 16%, and 13% for ZNBS1, 2, and 3, respectively.

Solution analysis

The element concentrations of leachate were measured by ICP-OES to investigate the quantity loss from the glass-water interaction.

Figure 2 presents the change of normalized mass loss of Si, B and Na with the increase of leaching time for both irradiated and original ZNBS series, respectively. The mass losses of three main elements Si, B and Na remain at a relatively low level for the Zr-doped quaternary borosilicate glass. The quantity of Zirconium loss is less than the detection limit of the measurement device. The leaching rate of the borosilicate glass is defined by[36]:

$$Q_i = \frac{C_i}{f_i\left(\frac{SA}{V}\right)} \quad (1)$$

$$NR_i = \frac{Q_i}{t} \quad (2)$$

where, Q_i represents the normalized quantity loss of the i element, in g m^{-2}; C_i is measured nuclide concentration in leachate, g L^{-1}; f_i is corresponding to the mass ratio of the i element in the pristine sample; SA is stand for surface area of the sample in contact with water and V for the volume of sample, with the unit of m^2 and m^3, respectively; NR_i represents the normalized dissolution rate of the i element, in g m^{-2} d^{-1}; and t is the leaching time in day.

The level of measurement uncertainties can vary depending on the specific test conditions, however, the measurement errors of Si, B, and Na concentrations, a relative standard deviation (RSD) of less than 5% was consistently observed across all conditions. For concentration measurement errors, it's crucial to consider additional sources of discrepancies. There are many other factors that should be taken into account for estimate the measurement error, for example, the volume deviations of the solution, and inconsistencies stemming from the leached samples, such as differences during sample preparation and irradiation, Ultimately, a relative uncertainty of less than 10% was determined for C_i.

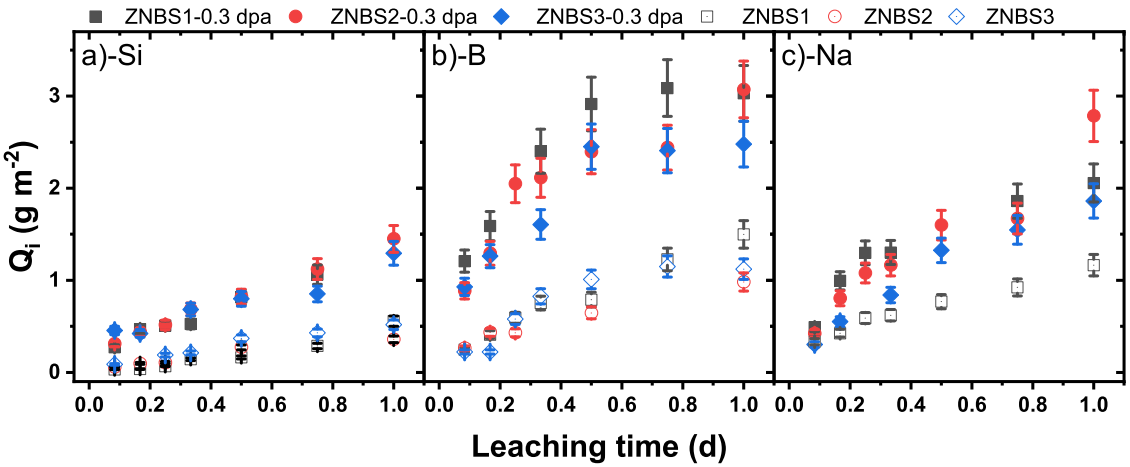

Fig. 2 Normalized quantity losses of different elements evolved with leaching time. The main element mass losses of Si, B, and Na for borosilicate glass are shown in (**a**–**c**), respectively.

The surface element distribution of leached sample

The XPS survey at the surface of the ZNBS series glass is present in Fig. 3. The element distribution of silicon remained relatively unchanged in the alter layer via SEM/EDS results as shown in Supplementary Figs. 2 and 3. Hence, the spectra were normalized by the intensity of Si ^{2}p. For both un- and irradiated ZNBS1, it is hard to find the signal related to the Na and B on the glass surface after leaching. The intensity of Si, and O remains relatively unchanged on the surface of the samples through the different time leaching.

Depth profile

The element distributions of H, O, Na, B, and Zr in ZNBS2 glass after leaching are observed by ToF-SIMS and shown in Figs. 4 and 5. The signals of listed elements were normalized to the signal of ^{28}Si. The leaching depth is characterized by the depth of half maximum value of Boron intensity after leaching, which should be in the interface of water-glass interaction. The thickness of alter layer induced by leaching are listed below in Table 1.

The behaviors of sodium and boron profile are changed simultaneously for irradiated sample as shown in Fig. 5, which all are opposite with the behavior of H, indicating that the Na and B were diffuse out due to the water-glass interaction and the H diffuse into the sample. The anticorrelated sigmoidal concentration profiles in the hydrated glass between Na/B and protons implied the domination of the interdiffusion during the initial time of water-glass interaction.

The black dash dot lines are calculated from the half maximum value of boron intensity represent the thickness of the alter layer for ZNBS2 glass with 0.3 dpa: (a) 426 nm for 2 h leaching; (b) 841 nm for 4 h leaching; (c) 1310 nm for 6 h leaching; (d) 1410 nm

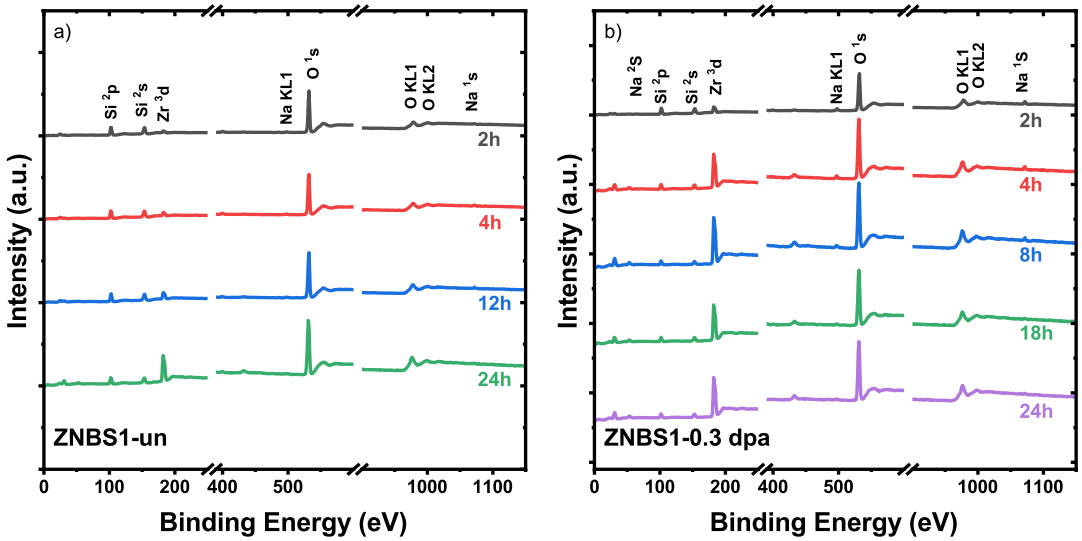

Fig. 3 XPS survey of un- and irradiated ZNBS1 after different time of leaching. a The un-irradiated ZNBS1; **b** ZNBS1 with 0.3 dpa.

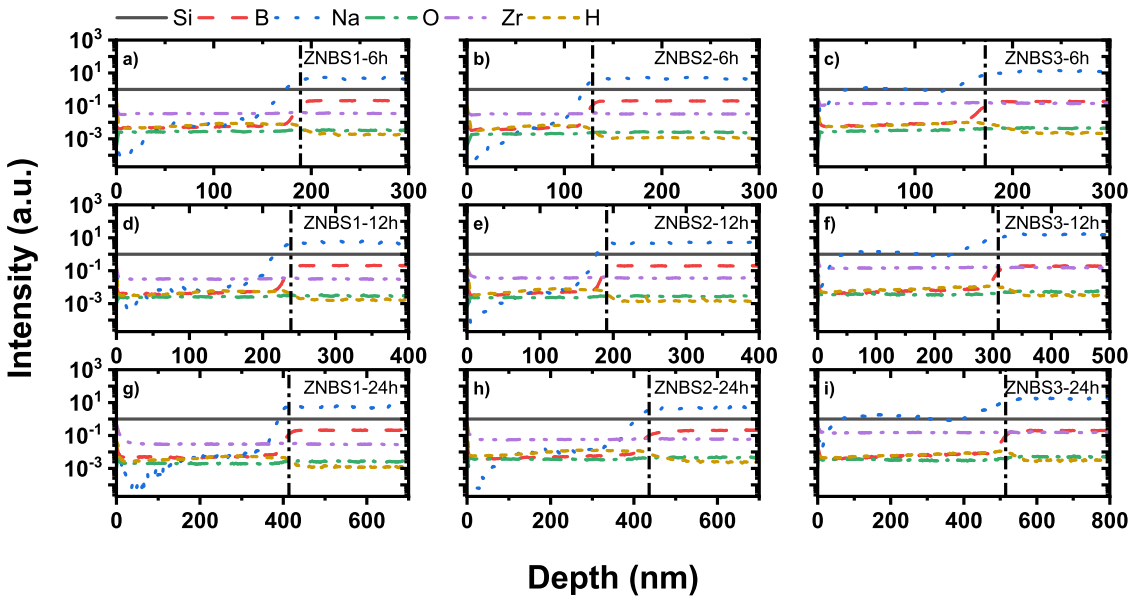

Fig. 4 Element distributions over the depth for un-irradiated ZNBS glasses after leaching. The black dash dot lines refer to the half maximum value of Boron intensity. **a**, **d**, **g** are the leaching profile for un-irradiated ZNBS1 glass after 6 h, 12 h, and 24 h leaching, respectively; **b**, **e**, **h** are the leaching profile for unirradiated ZNBS2 glass after 6 h, 12 h and 24 h leaching, respectively; **c**, **f**, **i** are the leaching profile for un-irradiated ZNBS3 glass after 6 h, 12 h and 24 h leaching, respectively.

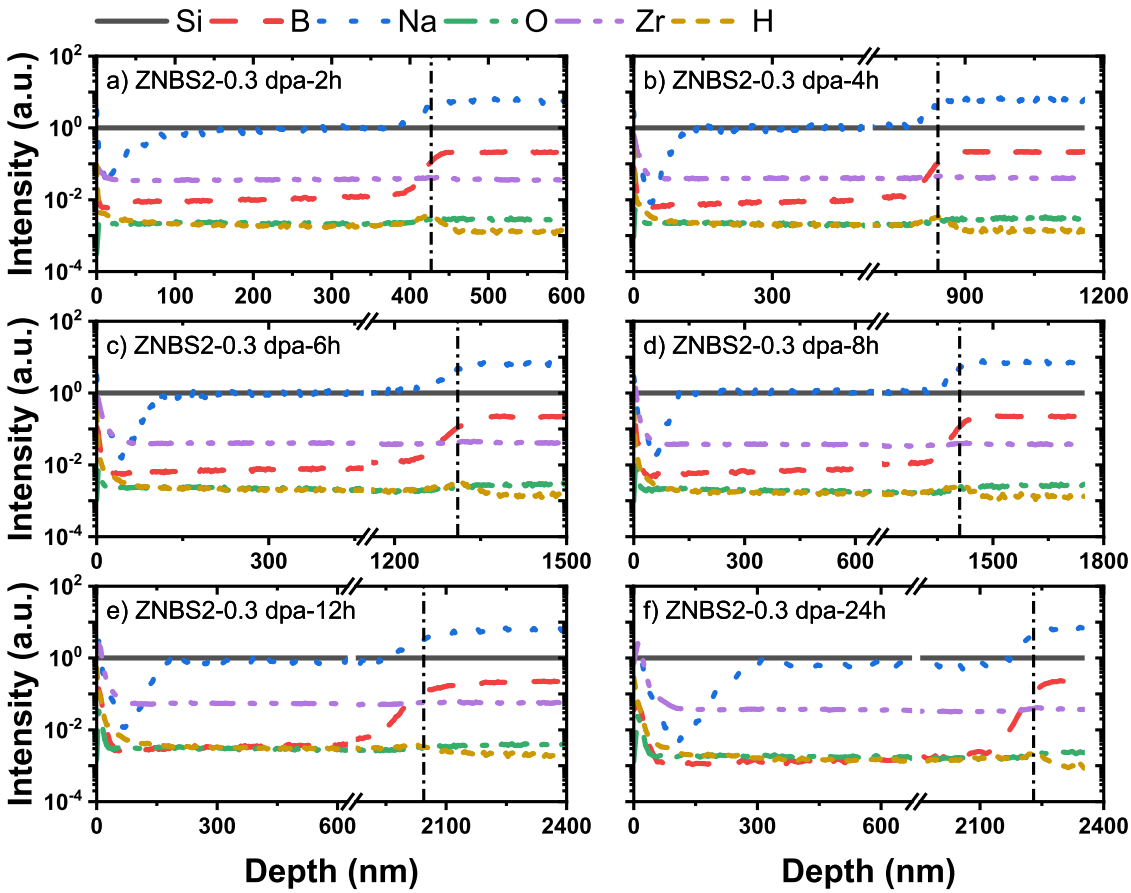

Fig. 5 Element distributions over the depth for ZNBS2-0.3 dpa after different leaching time. a–f are the individual distributions for ZNBS2-0.3 dpa after 2, 4, 6, 8, 12, 24 h of leaching, respectively. The black dot lines refer to the half maximum value of Boron intensity..

for 8 h leaching; (e) 2044 nm for 12 h leaching and (f) 2230 nm for 24 h leaching. The depth profile of ZNBS1-0.3 dpa and ZNBS3-0.3 dpa are shown in Supplementary Fig. 4 and 5, respectively.

Microstructure evolution

The FTIR spectra of ZNBS series glasses before and after irradiation with different leaching times are presented in Figs. 6 and 7, respectively. Since all experiments are conducted and all samples are measured at the same condition except for different leaching time, to analyze the microstructure changes quantitatively. All the spectra are the original infrared spectra.

The microstructure of ZNBS1 glasses underwent significant changes as the leaching time increased, as seen in Fig. 6. The primary changes observed are a gradual decrease in the $[BO_3]$-related structure and the progressive emergence of the peak at 1050 cm^{-1} corresponding to the Q^3 (O-Si-O) structure. Notably, the ZNBS1 glass which has lower Zr-doped content shows the most rapid change, while the ZNBS3 glass with higher Zr content is still in the process of slow formation of the structure at 1050 cm^{-1}.

The infrared spectra of the ion-irradiated ZNBS glass samples revealed a marked increase in the intensity of $[BO_3]$-related structures compared to the non-irradiated samples. This is attributed to the conversion of $[BO_4]$ units to $[BO_3]$ units during the ion irradiation process[36,40]. Over time, the leached samples exhibited more pronounced changes in their structural features compared to the control group. Specifically, the B-related structures on the surface of the ZNBS glass samples are almost completely leached out after 24 hours. The deconstruction of the B-O-B peak at 700 cm^{-1} after 6 hours of leaching results in the independent manifestation of the Si structure peak at 780 cm^{-1} for all ZNBS series samples. The changes in the area under the $[BO_3]$ region indicate that the $[BO_3]$ content in the ZNBS1 and ZNBS2 samples is rapidly leached out within 4 hours after irradiation, while the relatively mild area decrease for the 1250–1550 cm^{-1} region for ZNBS3 suggests that a certain amount of $[BO_3]$ still exists on its surface, likely due to its relatively high Zr content.

DISCUSSION

ICP-OES is a precise method for measuring the amount of elemental mass loss in borosilicate glass after leaching experiments. However, it may not provide a complete understanding of the impact of leaching on borosilicate glass, as the complex interplay between sample components and radiation effects can complicate interpretation. In contrast, FTIR spectroscopy is a highly sensitive and rapid method that clearly reveals the structural changes of both original and irradiated ZNBS series glass after interaction with water.

The initial leaching rates calculated from Si, B, and Na are listed in Table 2. For the pristine glass, the observed similar leaching rates of B and Na elements during the initial leaching stage imply that the ZNBS glass is significantly below the percolation threshold. Compared with the ternary system[36], the addition of zirconia into borosilicate glass significantly improved its water resistance. During the primary stage of leaching for the unirradiated ZNBS series samples, the mass loss of B and Na elements is higher than that of Si element, and their magnitudes are similar.

Table. 1. The thickness of boron interface measured by ToF-SIMS.

Time	Sqrt(t)	ZNBS1-un	ZNBS2-un	ZNBS 3-un	ZNBS1-0.3 dpa	ZNBS2-0.3 dpa	ZNBS3-0.3 dpa
h	$h^{1/2}$	nm					
2	1.4	—	—	—	359	426	252
4	2	—	—	—	—	841	596
6	2.5	189	128	170	—	1310	—
8	2.8	—	—	—	1552	1410	1079
12	3.5	237	189	307	—	2044	1251
18	4.2	—	—	—	2042	—	—
24	4.9	410	436	514	2135	2230	1720

For the irradiated samples, the interactions between the ZNBS glass and water were significantly enhanced. This was evident as the normalized mass loss of element B reached a saturation-like state after 8 hours of leaching, which should be due to the depletion of [BO_3] unit from the irradiation layer at this time (as shown in Fig. 7). Based on the B loss from the surface of the glass, the thickness of the ZNBS1 glass leached layer was estimated to be approximately 1.2 μm at this point. It is worth noting that the calculated thickness of the ZNBS1 water corrosion layer after 8 h leaching was found to be less than that of the irradiated damage layer caused by 5 MeV Xe^{20+} irradiation. Therefore, the initial leaching rate for irradiated borosilicate glass can be calculated by the linear regression upon 8 h of leaching. The initial leaching rate of Si, B and Na were fitted as listed in Table 2, and it was determined that the dissolution rates of Si of ZNBS1, 2, and 3 glasses were accelerated by 7.0 ± 2.5, 5.0 ± 1.3, and 3.5 ± 1.1 times, respectively, due to heavy ion irradiation.

Moreover, the normalized mass loss of these elements increased linearly with the square root of leaching time, as shown in Supplementary Fig. 6, indicating the dominance of the interdiffusion in the interaction between ZNBS series and water during the initial leaching phase[24].

The thickness of leached glass was represented by the depth of boron interface via ToF-SIMS. The corrosion layer had been accelerated significantly by the heavy ion irradiation. It is interesting that the alter layer changed only around 200 nm for ZNBS2-0.3 dpa while leaching from 12 h to 24 h as shown in Fig. 8. The black arrow in the Fig. 8 indicates the surged alteration in the thickness of corrosion layer results from the ion irradiation. The red arrows indicate the interaction between the pristine glass and the water.

Moreover, for un-irradiated ZNBS2 glass, the alter layer increased to around 190 nm on its first 12 h water corrosion. The observed minimal variation in the thickness of the altered layer between the 24-hour and 12-hour ZNBS2-0.3 dpa samples could be a consequence of the interaction between water and the pristine glass matrix. This subtle change in thickness can serve as empirical evidence supporting the estimated depth of the irradiated layer as determined by SRIM calculations. This correlation between experimental observation and SRIM estimations reinforces the validity of the predicted irradiation depth within the glass structure. This finding provides an explanation for the saturation-like state observed in the boron normalized mass loss, as depicted in Fig. 2.

For the pristine glasses, the changing rate of all three types of ZNBS glasses on boron interface shows a similar water resistance in the initial leaching stage. However, it is interesting to find that the element interface of boron is slight deeper than the interface of sodium in around 10 nm, which might be caused by two interactions: (a) the solid-water diffusion: the leaching out of [BO_3] unit which left the void to be filled with H_2O; (b) the ion exchange between the sodium ion with the H^+, which results from two source: the transformation from [BO_4] to [BO_3] and the losing sodium from Q^n species. In glass network, sodium ions serve as the charge-compensating element around the [BO_4] unit and Q^n species. In water-glass interaction, the loss of sodium by ion exchange results in the transformation of surrounding [BO_4] units to [BO_3] units, which further leads to a solid-water diffusion of [BO_3]. This space is subsequently occupied by water, which could account for the observed phenomenon of unsynchronized element leaching. After irradiation, most of the [BO_4] converted to [BO_3]. As a result, the corrosion behavior of both sodium and boron elements occurred simultaneously, as depicted in Fig. 5. Further investigation in the acid leachate may help verify the above assumption.

Moreover, on the surface of leached ZNBS glasses for both irradiated and un-irradiated glasses, the enrichment of Zirconium was found via both ToF-SIMS and XPS analysis. The increased intensity of Zr peak around the surface might because Zr is the element almost completely retained in the water corrosion layer[41].

After the ZNBS series glass samples contacted with water, a new structure associated with water appeared at 1633 cm^{-1} in all FTIR spectra of the leached samples, as shown in Fig. 9, which was not present in the original un-leached samples. Figure 9 presents the corresponding area of the peak 1633 cm^{-1} which attributed from the water content of the ZNBS glass surfaces[42].

The rate of change in water content for ZNBS1 and ZNBS2 was similar regardless of the radiation. For the unirradiated samples, the similar increase rate of the water-related structure may result from the Na_2O/B_2O_3 molar ratio being the same in ZNBS1 and ZNBS2, which suggests a strong correlation between the leaching of sodium (Na) and boron (B) elements and the intrusion of water into the glass matrix. For un-irradiated ZNBS3 glass, the water-related structure after leaching is higher than ZNBS1 and ZNBS2, which is consistent with ToF-SIMS results.

The water content in the samples after leaching showed a linear correlation with the square root of time, suggesting a diffusion-controlled process. Comparing the results of ZNBS 1, 2 and 3, it was found that the rate of change in water content increased by 3.4, 4.1, and 2.5 times, respectively, due to irradiation. The radiation effect on ZNBS series leaching analyzed from FTIR spectra is consistent with the element loss result from ICP-OES, as shown in Fig. 2.

Based on the IR spectra of ZNBS series glasses, it is evident that the most significant impact of irradiation on the quaternary borosilicate glass is the rise in IR absorption spectrum at 1250–1550 cm^{-1}, indicating an increase in [BO_3] units in the glass after irradiation. To qualitatively comprehend the change in [BO_3] units due to leaching, a multi-Gaussian fitting was conducted on the structure of [BO_3] units in the IR spectrum of each leaching, and the fitting scheme is shown in the inset plot in Fig. 10.

The change in [BO_3] after irradiation reflects the damage of irradiation on the leaching resistance of borosilicate glass, in addition to the fact that this effect varies according to the component differences. The rate of [BO_3]-related intensity change

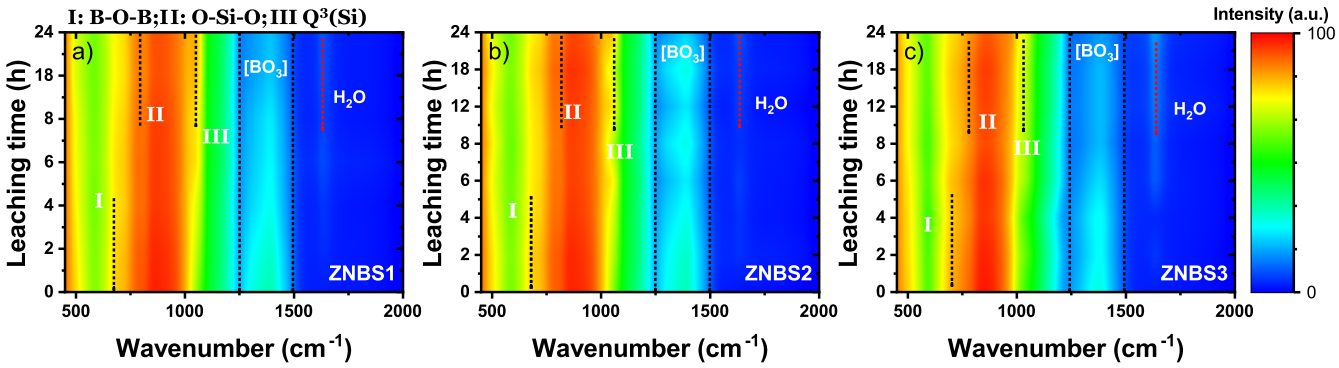

Fig. 6 FTIR colormaps of non-irradiated ZNBS samples evolved with different leaching time. a–c are the corresponding FTIR colormap for ZNBS1, ZNBS2 and ZNSB3 evolved with leaching time, respectively. Three peaks labeled as Roman numerals I, II, and III, correspond to the B-O-B structure at approximately 700 cm^{-1}, the O-Si-O structure at around 780 cm^{-1}, and the Si-related Q structure at approximately 1050 cm^{-1}, respectively.

increased 4.1 ± 0.8, 5.3 ± 1.5, and 2.5 ± 0.6 times for ZNBS1, 2 and 3, respectively.

After the analysis of water content and $[BO_3]$ unit change, it is interesting to find the relation between the change of $[BO_3]$ unit and surface water content of ZNBS series. As shown in Fig. 11, the $[BO_3]$ content shows an inverse relationship with the water-related structure during leaching for the unirradiated glass. Compared to the results from ToF-SIMS and the SRIM simulation, the alter layer reached around 2000 nm at 12 h leaching and the designed irradiated layer is around 1.72 µm for ZNBS1. The disappearance of $[BO_3]$ signal indicates that the structure of BO_3 leached out from the ZNBS glass surface, the void left by it was filled by molecular water. This relationship also held for the irradiated samples, where the $[BO_3]$ in the irradiation layer was completely leached out, resulting in the area of the FTIR spectrum associated with it tending towards 0. Simultaneously, the area under the peak of the water-related structure tended to saturate, indicating that the pores of the surface $[BO_3]$ structure were filled by water from the leaching solution. This effect suggested that the decrease in $[BO_3]$ structure due to leaching could promote the formation of water-related structures on the glass surface. Therefore, the analysis of water related structure in leaching layer could help characterize the leaching resistance of borosilicate glass.

Without leaching, the Si-related peaks at 780 cm^{-1} or 1050 cm^{-1} were not clearly distinguishable in the initial FTIR spectra of both unirradiated and irradiated samples as shown in Fig. 6 and Fig. 7, respectively. However, as the glass soaked in water, the relative intensity of the peak at 780 cm^{-1}, which corresponding to O-Si-O vibration, increased with the square root of leaching time, as illustrated in Fig. 12. For the ions-irradiated glasses, the area of Si-related peak as 780 cm^{-1} increases with the leaching time, due to the loss of B-relating background[43] at around 700 cm^{-1}. In order to separate the peak of O-Si-O vibration (780 cm^{-1}) and Si-related Q^3 (1050 cm^{-1}) from the FTIR spectra ranging from 600 to 1250 cm^{-1}, the FTIR spectra of un-leached samples were chose as the background information. The changes in the areas of O-Si-O vibration and Si-related Q^3 structure were obtained by the Difference-in-Differences (DiD) method, which generally using the FTIR spectrum of leached sample to subtract the background information as shown in Supplementary Fig. 7.

During the initial stage of leaching, it was observed that there was no significant change in the peaks related to the silicon network structure as the leaching time increased, as shown in Fig. 12. This finding indicates that the interaction between the ZNBS glasses and water is primarily characterized by the disintegration of the boron network structure due to the diffusion effects. In contrast to the noticeable changes observed in the $[BO_3]$ region, as discussed above, the peaks related to the silicon network structure remained relatively stable, suggesting that the silicon network structure is less prone to degradation during the early stages of leaching. The relatively low value of 780 cm^{-1} peak area of unirradiated ZNBS3 should result from its composition as listed in Table 3.

Figure 12 shows the evolution trends of the area of 780 cm^{-1} peak with the square root of leaching time. As the leaching of the boron structure at 700 cm^{-1} proceeds rapidly, the Si-related peak areas of irradiated ZNBS1 and ZNBS2 reach saturation-like state after 8 hours, indicating that the dissolution of the silicon network structure is relatively slower than that of the boron network structure. This trend is consistent with the behavior of the $[BO_3]$ and water structures, suggesting that the interaction between the ZNBS glasses and water is primarily driven by the diffusion of boron species. The relatively more leaching-resistant behavior of elemental Si in the initial stage can be attributed to its stronger covalent bond with oxygen, which hinders its dissolution in water[36,44].

However, in the case of irradiated ZNBS3, the area under the peak of the Si-related structure continued to show a linear relationship with the square root of time, even after prolonged leaching. This indicates that the B-structure at 700 cm^{-1} in ZNBS3 has not been leached out. This may be due to the higher Zr content in ZNBS3, which can inhibit part of the hydrolysis rate of the B network, resulting in a slower leaching rate and a longer leaching time required to fully disintegrate the boron network. This result is also consistent with the thickness change of corrosion layer by ToF-SIMS as shown in Fig. 8.

Figure 13 presents the relation between the B and Si related structure of the leached ZNBS glass surface before and after radiation. For the unirradiated ZNBS samples, it was observed that the surface B and Si-related structures were inversely correlated after leaching. This phenomenon can be attributed to the fact that the background signal results from the B structure around the Si-related structures ranging from 600-720 cm^{-1} was also being leached out. As a result, the O-Si-O tensile vibration at the 780 cm^{-1} was more visible while the time increased.

The effect of irradiation on the leaching of B-related structures was significant, resulting in an accelerated leaching rate. Therefore, the Si-related structures in the irradiated leached samples exhibited significant changes, which were primarily due to the decrease in leaching resistance resulting from irradiation. This suggests that the irradiation had a strong impact on the stability of the boron network of the glass, leading to a change in the leaching behavior of the B-related structures.

Figure 14 depicts the correlation between the $[BO_3]$ structure from the FTIR analysis of the glass surface and the normalized quantity loss of element B in the leachate measured by ICP-OES. For the pristine borosilicate glass, the water-glass interaction is dominated by the diffusion phenomena. Therefore, the $[BO_3]$

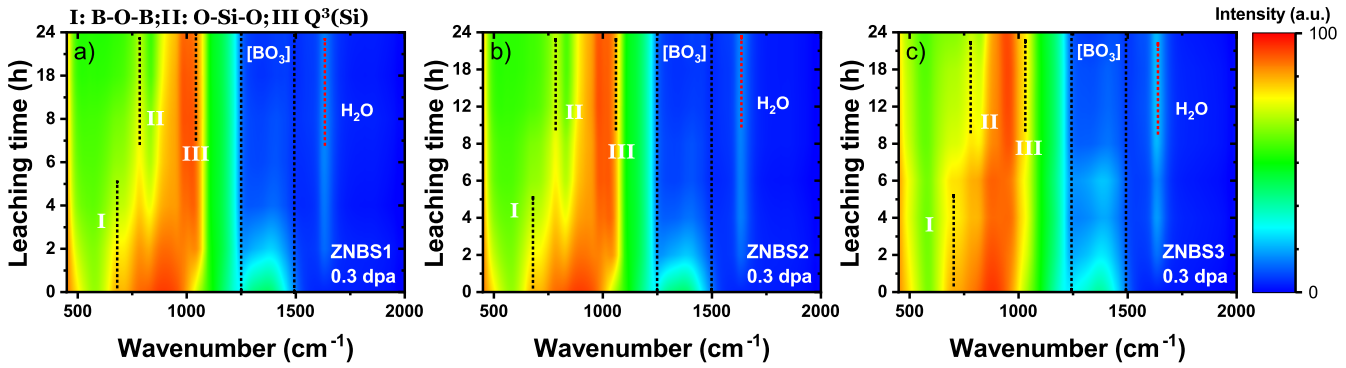

Fig. 7 FTIR colormaps of irradiated ZNBS samples evolved with different leaching time. a–c are the corresponding FTIR colormaps for irradiated ZNBS1, ZNBS2 and ZNSB3 evolved with leaching time, respectively. Three peaks labeled as Roman numerals I, II, and III, correspond to the B-O-B structure at approximately 700 cm^{-1}, the O-Si-O structure at around 780 cm^{-1}, and the Si-related Q structure at approximately 1050 cm^{-1}, respectively.

Table. 2. The initial leaching rate of ZNBS series obtained from linear regression[a].

Sample	$r_{0\text{-}Si}$ (g m^{-2} d^{-1})	$r_{0\text{-}B}$ (g m^{-2} d^{-1})	$r_{0\text{-}Na}$ (g m^{-2} d^{-1})
ZNBS1	0.3 ± 0.1	1.9 ± 0.2	1.6 ± 0.2
ZNBS2	0.5 ± 0.1	1.4 ± 0.3	1.3 ± 0.3
ZNBS3	0.6 ± 0.1	1.7 ± 0.3	1.4 ± 0.3
ZNBS1-0.3 dpa	2.1 ± 0.3	9.1 ± 1.3	4.9 ± 0.5
ZNBS2-0.3 dpa	2.5 ± 0.4	8.5 ± 0.8	4.7 ± 0.3
ZNBS3-0.3 dpa	2.1 ± 0.5	5.7 ± 1.1	2.9 ± 0.3

[a]The R^2 for all linear regression are better than 0.85.

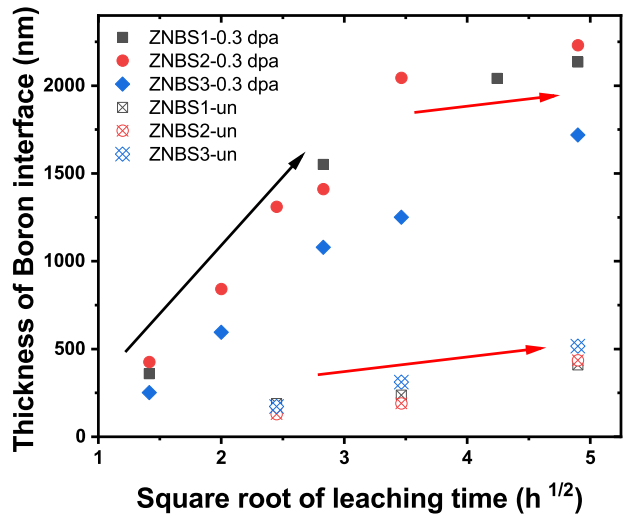

Fig. 8 The thickness of Boron diffusion interface involved with square root of leaching time. The black arrow indicates the accelerated water-glass interaction results from the ion irradiation. The red arrows indicate the interaction between the pristine glass and the water.

structure in the surface of borosilicate glass measured by the FTIR can reflect the remaining Boron element in the alter layer of the glass.

Each set of data is normalized by its initial value. The plot shows that in the initial stages of leaching, these two physical quantities are inversely related and exhibit similar trends.

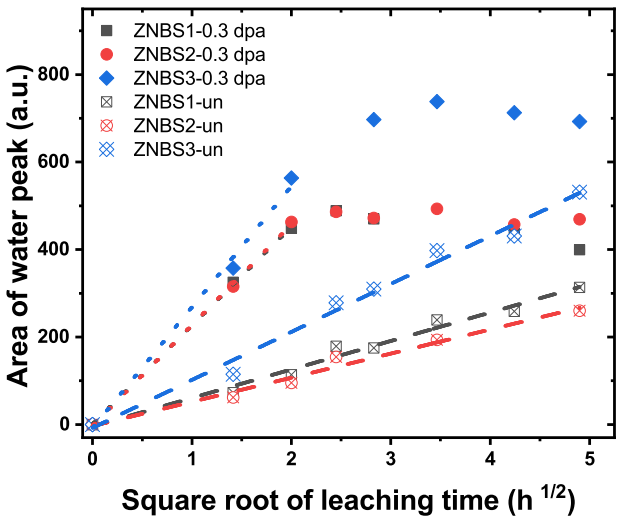

Fig. 9 The area of water related structure from FTIR spectra of ZNBS series glasses evolved with leaching time. The dot lines represent the linear region for irradiated sample and dashed lines for un-irradiated samples. The surface water intensity from FTIR increases linearly with the square root of time for un-irradiated samples. For irradiated sample, the surface water intensity shows similar trend at first few hours leaching and then changes to a saturated-like state for the following leaching.

Furthermore, the correlation between the $[BO_3]$ structure in the FTIR analysis of the glass surface and the normalized mass of element B in the leachate measured by ICP-OES confirms the interplay between the leaching of the $[BO_3]$ structure and the release of element B into the leachate. This relationship suggests the existence of a coefficient that allows for the conversion of the relationship between the measured concentration by OES and the relative change of intensity of the $[BO_3]$ structure by FTIR analysis as:

$$Q_B = 2.13(\pm 0.1) \times RI_i \tag{3}$$

where RI_i is the relative change of intensity of $[BO_3]$ after leaching i hours in the surface of the glass, given by:

$$RI_i = \frac{(I_0 - I_i)}{I_0} \tag{4}$$

where I_0 is the intensity of $[BO_3]$ structure from FTIR spectrum.

In this work, the effects of components and irradiation on the leaching behavior of quaternary borosilicate glasses with varying zirconium contents were investigated by SEM/EDS, XPS, ToF-SIMS,

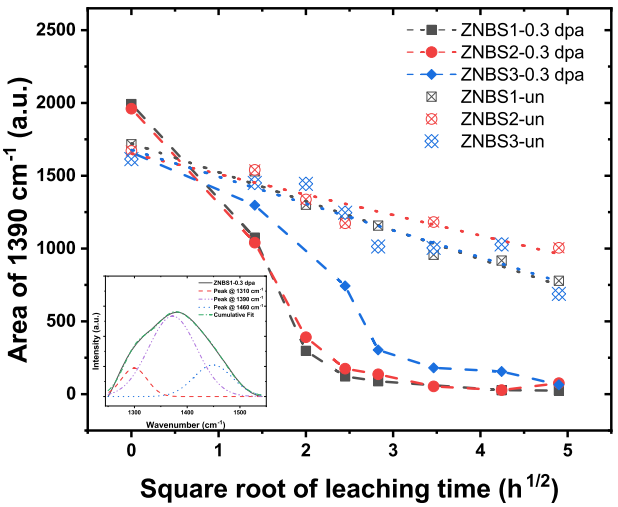

Fig. 10 The change of [BO_3]-related structure with square root of leaching time, the inset plot is a typical three peak Gaussian fitting for the [BO_3] unit ranging from 1250 to 1550 cm^{-1}. The dot lines represent the linear region for irradiated sample and dashed lines for un-irradiated samples. For Pristine glass, the surface [BO_3] leached out linearly with the increase of the square root of leaching time. After ion irradiation, the loss of [BO_3] had been significantly accelerated.

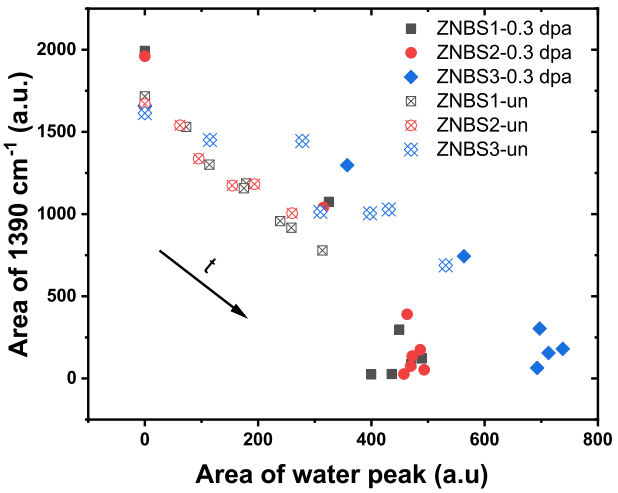

Fig. 11 The relation between the BO_3 unit and surface water of ZNBS series with leaching time. The black arrow indicates the leaching time flow. For the pristine ZNBS glasses, the loss of [BO_3] due to the leaching is anticorrelated with the increase of the surface water content.

ICP-OES and FTIR measurement. The element distributions at the cross-section of irradiated glass cannot observe any significant change after leaching via SEM/EDS. XPS results indicated that there was no signal related to the Na and B in the surface 15 nm of glass samples after leaching. The depth profiles of irradiated ZNBS glass after leaching was measured by ToF-SIMS. The anticorrelated sigmoidal concentration profiles in the hydrated glass between Na/B and protons indicated the interdiffusion process. The alter layers for irradiated ZNBS glasses exceed the designed irradiation layer after 12 hours of leaching. Comparing the depth of un-irradiated and irradiated ZNBS2 glass after 6 hours of leaching, there is a significant increase in approximately 7 times resulting from the ion irradiation.

For the un-irradiated glasses, the linear trends of elemental mass loss on square root of time indicated that the initial stage of

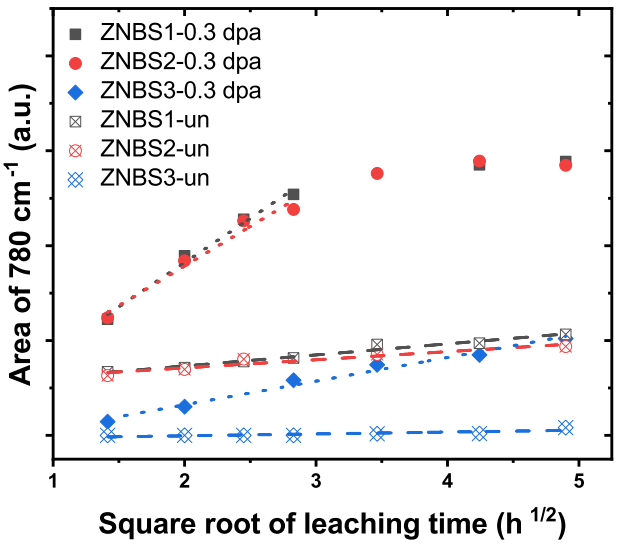

Fig. 12 The changes in O-Si-O stretching vibration for different glasses evolved with leaching time. The dot lines represent the linear region for irradiated sample and dashed lines for un-irradiated samples. For the pristine glass, the changes in the Si-related structure are tenuous, and the change of Si peak are even less pronounced at higher Zr contents. After irradiation, the Si peak appears due to the leaching of Boron. Meanwhile, differences in rates of Si peak change imply differences in ZNBS glass compositions.

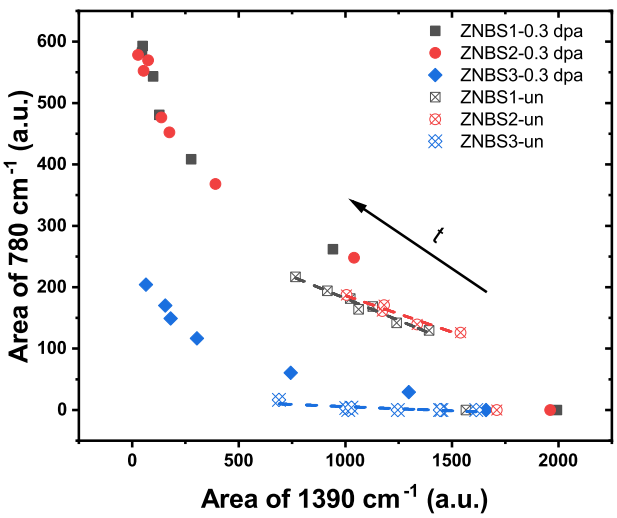

Fig. 13 The relation between the [BO_3] unit of peak 1390 cm^{-1} and Si-O-Si structure at of peak 780 cm^{-1}. The dashed lines for the linear correlation region between the Si- and B- related structure for un-irradiated samples. The black arrow indicates the leaching time flow.

water-glass interaction was dominated by the diffusion phenomenon. As the borosilicate glass underwent leaching, the dissolution of B-related structures might lead to the formation of many micropores on the glass surface which had been observed by other works[23,45]. These micropores were then filled with the leaching solution, resulting in the appearance of water-related absorbance peak of FTIR spectrum on the sample's surface after leaching. Simultaneously, the loss of B element results in the appearance of Si-related structure at 780 cm^{-1} from FTIR spectrum. For the unirradiated glass, the initial stage of leaching is primarily driven by diffusion. At this stage, the leaching of [BO_3]

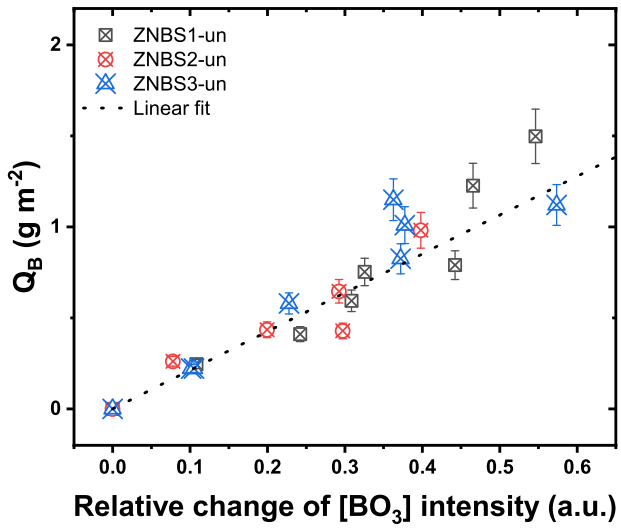

Fig. 14 The relation between the intensity of [BO_3] units in un-irradiated glasses and the B concentration at their leachate, all data has been normalized by its initial value. The change of boron intensity from FTIR analysis is correlated with the normalized mass loss from ICP-OES measurements, which provide an alternative method for examining the leaching behavior of borosilicate glass.

units, the intrusion of water, and the exposure of silicon structures occur simultaneously, and their behaviors are interconnected.

The similar value of initial leaching rate for ZNBS series reflects the impassivity of ICP-OES in investigating the composition effect on leaching behaviors of borosilicate glass. The resistance of water intrusion into the surface of ZNBS glass may exhibit an increase as the *R* value increases from the result of FTIR analysis. Furthermore, the resistance of Boron element loss is expected to increase with higher concentrations of Zirconium (Zr) in the glass.

The leaching behavior of the ZNBS series glass was observed to be significantly accelerated by ion radiation. Structural analysis using FTIR and ICP-OES techniques on the irradiated samples indicated that the loss of [BO_3] follows the diffusion law. Ion radiation resulted in the formation of a 1.72 μm radiation layer, leading to an increase in the [BO_3] unit on the surface of the ZNBS series. This enlargement of the contact interface between water and irradiated glass intensified the interaction between them. The initial leaching rate of Si for ZNBS1, ZNBS2, and ZNBS3 increased by 7.0 ± 2.5, 5.0 ± 1.3, and 3.5 ± 1.1 times, respectively, after irradiation. Furthermore, the peak analysis of the FTIR spectrum provided valuable insights into the impact of ion irradiation on the leaching behavior of the ZNBS series. It revealed that, after irradiation, the intensity change rate of the [BO_3]-related structure over square root of leaching time increased by 4.1 ± 0.8, 5.3 ± 1.5, and 2.5 ± 0.6 times for ZNBS1, ZNBS2, and ZNBS3, respectively. This signifies a remarkable alteration in the leaching behavior of the glass samples due to the influence of ion irradiation as well as the result from ICP-OES.

Furthermore, the FTIR analysis showcased its high sensitivity in examining the composition and irradiation effects of borosilicate glasses. The immediate FTIR measurements performed after leaching served as a direct means to observe the alterations taking place in the surface structure as a consequence of leaching. These real-time measurements can be regarded as in-situ IR measurements, providing valuable insights into the dynamic behavior of the glass during leaching processes. Additionally, a direct conversion method was established, enabling the transformation of ICP-OES results into IR measurements by fitting the relationship between the variation in [BO_3] and the concentration of B-elements in the leaching solution.

Table. 3. The compositions of the Zr doped borosilicate glasses.

mol%	SiO_2	B_2O_3	Na_2O	ZrO_2	$R = Na_2O/B_2O_3$	$K = SiO_2/B_2O_3$	ρ (g/cm^3)
ZNBS1	60.20	19.80	18.30	1.70	0.92	3.04	2.51
ZNBS2	55.00	21.88	20.13	3.00	0.92	2.51	2.52
ZNBS3	50.00	16.45	29.05	4.50	1.77	3.04	2.72

METHODS

Glass preparation

The glass recipes used in this work are based on the ternary borosilicate glass with adding different mass ratio of zirconia as shown in Table 3.

The Zr-doped borosilicate glasses, as annotated as ZNBS series, was fabricated using a melting-annealing process and then cut into rectangular pieces with dimensions of 10 mm × 10 mm × 1 mm[40]. To ensure the quality of the samples, both sides of each piece were carefully polished to achieve a fine surface roughness. The purpose for the ZNBS series is to investigate the effect of zirconia on the leaching behavior of borosilicate glass.

Irradiation experiment

The ZNBS series were subjected to ion irradiation using a 5 MeV Xe^{20+} beam from the 320 kV multi-discipline research platform located at the China Academy of Sciences Institute of Modern Physics in Lanzhou. The irradiation was carried out of a fluence 2×10^{14} ions cm^{-2} on one side of the glass to simulate the damage of recoil nucleus, corresponding to dose of 0.3 dpa[21]. The designed irradiation layer in the surface of ZNBS 1 and 2 is approximately 1.72 μm, and the one for ZNBS3 is around 1.60 μm calculated by SRIM simulation[46].

Leaching experiment

The leaching behavior of the irradiated ZNBS glass was investigated using the MCC-1 static leaching method[47] at the temperature of 90 °C. Since the most of our studies are performed in pure water equilibrated with the atmosphere, the leachate is using the deionized water saturated with CO_2 from air and the pH=6.5 (25 °C). The ratio of the leachate volume to surface area of the glass was 15 cm. The irradiated glass samples were immersed in the leachate within a hydrothermal reactor lined with polytetrafluoroethylene (PTFE) for varying lengths of time, ranging from 2 to 24 h, in order to study the initial stage of leaching while taking into account the thickness of the irradiation layer. The pristine samples were used as the control group to evaluate the radiation effect on the leaching behavior of the glass. Considering the measurement of ATR-FTIR will apply a force on the surface of glass leading to the change the surface area, each data point uses individual specimens. Specifically, for a set of data comprising eight points (for 0, 2, 4, 6, 8, 12, 18, and 24 h leaching), eight concurrently prepared specimens were subjected to leaching tests, all under consistent conditions but spanning different durations.

Solution analysis

Inductively Coupled Plasma-Optical Emission Spectroscopy (ICP-OES) was used to measure the nuclide contents in leaching solution. The ICP-OES instrument was the Plasma Quant PQ 9000 Elite, manufactured by Analytik Jena in Jena, Germany.

Microstructure analysis

All samples used in this experiment were prepared and irradiated under identical conditions to reduce system uncertainties. The

surface analysis was conducted on samples that were removed from leaching vessel at a specific leaching time and then using analytical filter paper to absorb the moisture from the sample surface at room temperature before analyzing the surface.

The Fourier transform infrared (FTIR) spectra of the samples were obtained on the attenuated total reflectance (ATR) Perkin-Elmer Spectrum II spectrophotometer. The spectra were collected by 11 scans in the wavenumber range of 450–4000 cm^{-1} and subtracted the background information including H_2O and CO_2 from the atmosphere, with a resolution of 4 cm^{-1}. Each sample was conducted to the diamond reflector and measured at three different areas to ensure the repeatability of the FTIR spectra as shown in Supplementary Fig. 1. The ATR-FTIR technique allows for direct analysis of the sample surface, making it ideal for studying leaching behavior. The depth probed by ATR-FTIR under these conditions are less than 1.75 μm while wavenumber larger than 1200 cm^{-1}. The collected spectra were then analyzed to identify changes in the microstructure of the glass as a result of irradiation and leaching.

Leaching profile

X-ray Photoelectron Spectroscopy (XPS, ESCALAB Xi^+, Thermo Fisher Scientific) was employed to investigate the surface element for ZNBS series after leaching. The probed depth of XPS measurement is 15 nm.

The time-of-flight flight secondary ion mass spectrometry (ToF-SIMS, IONTOF GmbH) was employed to investigate the alter layer of ZNBS series glass after leaching at a certain time. The samples were pumped overnight to ensure the vacuum level of 10^{-7} Pa during the measurement. The $O_2{}^+$ raster size for depth profiling was set to 300 × 300 μm^2. The analysis utilized a 25 keV monatomic Bi^+ beam (~1.0 pA) operating at a 10 kHz frequency. Depths were gauged using a profilometer, correlating linearly with sputtering time. Positive ions were selected for analysis, and a floodgun was used throughout to counteract any charging effect.

DATA AVAILABILITY

The data used in this study is available from the corresponding author upon reasonable request.

Received: 31 May 2023; Accepted: 4 January 2024;
Published online: 17 January 2024

REFERENCES

1. Ewing, E. C., Weber, W. J. & Clinard, F. W. Radiation effects in nuclear waste forms for high-level radioactive waste. *Prog. Nucl. Energy* **29**, 63–127 (1995).
2. Gin, S. et al. An international initiative on long-term behavior of high-level nuclear waste glass. *Mater. Today* **16**, 243–248 (2013).
3. Goel, A., McCloy, J. S., Pokorny, R. & Kruger, A. A. Challenges with vitrification of Hanford High-Level Waste (HLW) to borosilicate glass–An overview. *J. Non-Cryst. Solids X* **4**, 100033 (2019).
4. Zhang, Y. & Mir, A. H. A review of brannerite structured materials for nuclear waste management. *J. Nucl. Mater.* **583**, 154512 (2023).
5. Weber, W. J. Radiation effects in nuclear waste glasses. *Nucl. Instrum. Meth B* **32**, 471–479 (1988).
6. Weber, W. J. et al. Radiation effects in glasses used for immobilization of high-level waste and plutonium disposition. *J. Mater. Res.* **12**, 1946–1978 (1997).
7. Mir, A. H. Using external ion irradiations for simulating self-irradiation damage in nuclear waste glasses: State of the art, recommendations and, prospects. *J. Nucl. Mater.* **539**, 152246 (2020).
8. Gin, S., Jollivet, P., Tribet, M., Peuget, S. & Schuller, S. Radionuclides containment in nuclear glasses: an overview. *Radiochim. Acta* **105**, 927–959 (2017).
9. Malkovsky, V. I., Yudintsev, S. V., Ojovan, M. I. & Petrov, V. A. The influence of radiation on confinement properties of nuclear waste glasses. *Sci. Technol. Nucl. Install.* **2020**, 8875723 (2020).
10. Burns, W. G., Hughes, A. E., Marples, J. A. C., Nelson, R. S. & Stoneham, A. M. Radiation effects and the leach rates of vitrified radioactive waste. *Natur* **295**, 130–132 (1982).
11. Peuget, S. et al. Effects of deposited nuclear and electronic energy on the hardness of R7T7-type containment glass. *Nucl. Instrum. Meth B* **246**, 379–386 (2006).
12. Utton, C. A. et al. Dissolution of vitrified wastes in a high-pH calcium-rich solution. *J. Nucl. Mater.* **435**, 112–122 (2013).
13. Peuget, S. et al. Comparison of radiation and quenching rate effects on the structure of a sodium borosilicate glass. *J. Non-Cryst. Solids* **378**, 201–212 (2013).
14. Mir, A. H. et al. Defect recovery and damage reduction in borosilicate glasses under double ion beam irradiation. *Epl-Europhys. Lett.* **112**, 36002 (2015).
15. Chen, L. et al. Study of modifications in the mechanical properties of sodium aluminoborosilicate glass induced by heavy ions and electrons. *Nucl. Instrum. Meth B* **370**, 42–48 (2016).
16. Peng, H. B. et al. Effect of irradiation on hardness of borosilicate glass. *J. Non-Cryst. Solids* **443**, 143–147 (2016).
17. Wang, T. S. et al. Morphological study of borosilicate glass surface irradiated by heavy ions. *Surf. Coat. Tech.* **306**, 245–250 (2016).
18. Mir, A. H., Monnet, I., Boizot, B., Jégou, C. & Peuget, S. Electron and electron-ion sequential irradiation of borosilicate glasses: impact of the pre-existing defects. *J. Nucl. Mater.* **489**, 91–98 (2017).
19. ZHANG, X.-Y. et al. Mechanical properties of borosilicate glass with different irradiation of heavy ions. *J. Inorg. Mater.* **34**, 741–747 (2019).
20. Lv, P. et al. Composition-dependent mechanical property changes in Au-ion-irradiated borosilicate glasses. *J. Nucl. Mater.* **520**, 218–225 (2019).
21. Chen, L. et al. Radiation effects on structure and mechanical properties of borosilicate glasses. *J. Nucl. Mater.* **552**, 153025 (2021).
22. Zubekhina, B. Y., Burakov, B. E. & Ojovan, M. I. Surface alteration of borosilicate and phosphate nuclear waste glasses by hydration and irradiation. *Challenges* **11**, 14 (2020).
23. Mir, A. H. et al. Effect of decades of corrosion on the microstructure of altered glasses and their radiation stability. *npj Mater. Degrad.* **4**, 11 (2020).
24. Frugier, P. et al. SON68 nuclear glass dissolution kinetics: current state of knowledge and basis of the new GRAAL model. *J. Nucl. Mater.* **380**, 8–21 (2008).
25. Geisler, T. et al. Aqueous corrosion of borosilicate glass under acidic conditions: a new corrosion mechanism. *J. Non-Cryst. Solids X* **356**, 1458–1465 (2010).
26. Ojovan, M. I., Hand, R. J., Ojovan, N. V. & Lee, W. E. Corrosion of alkali–borosilicate waste glass K-26 in non-saturated conditions. *J. Nucl. Mater.* **340**, 12–24 (2005).
27. Qin, K. M. et al. Composition-dependent leaching behavior in ion-irradiated borosilicate glasses: a corrosion mechanism study. *J. Am. Ceram. Soc.* **107**, 859–870 (2024).
28. Ebert, W. L., Bates, J. K., Buck, E. C. & Bradley, C. R. Accelerated glass reaction under PCT conditions. *OPL* **294**, 569–576 (1992).
29. Vienna, J. D., Ryan, J. V., Gin, S. & Inagaki, Y. Current understanding and remaining challenges in modeling long-term degradation of borosilicate nuclear waste glasses. *Int. J. Appl. Glass Sci.* **4**, 283–294 (2013).
30. Chave, T., Frugier, P., Ayral, A. & Gin, S. Solid state diffusion during nuclear glass residual alteration in solution. *J. Nucl. Mater.* **362**, 466–473 (2007).
31. Geneste, G., Bouyer, F. & Gin, S. Hydrogen-sodium interdiffusion in borosilicate glasses investigated from first principles. *J. Non-Cryst. Solids* **352**, 3147–3152 (2006).
32. Gin, S. et al. Effects of irradiation on the mechanisms controlling the residual rate of an alumino-borosilicate glass. *npj Mater. Degrad.* **6**, 59 (2022).
33. Mougnaud, S. et al. Heavy ion radiation ageing impact on long-term glass alteration behavior. *J. Nucl. Mater.* **510**, 168–177 (2018).
34. Peuget, S., Tribet, M., Mougnaud, S., Miro, S. & Jégou, C. Radiations effects in ISG glass: from structural changes to long-term aqueous behavior. *npj Mater. Degrad.* **2**, 1–9 (2018).
35. Tribet, M. et al. New insights about the importance of the alteration layer/glass interface. *J. Phys. Chem. C* **124**, 10032–10044 (2020).
36. Zhang, X. et al. Influence of ion radiation on leaching behavior of borosilicate glass. *J. Non-Cryst. Solids* **602**, 122091 (2023).
37. Chen, L. T. et al. Changes in macroscopic and microscopic properties of borosilicate glass irradiated with ions. *Radiat. Eff. Defect S* **176**, 789–803 (2021).
38. Wan, J. P., Cheng, J. S. & Lu, P. The coordination state of B and Al of borosilicate glass by IR spectra. *J. Wuhan. Univ. Technol.* **23**, 419–421 (2008).
39. Tenney, A. & Wong, J. Vibrational spectra of vapor-deposited binary borosilicate glasses. *J. Chem. Phys.* **56**, 5516–5523 (1972).
40. Yang, F. et al. Evaluation of nuclear transmutation effects due to beta decay on borosilicate glasses. *Int J. Appl Glass Sci.* **14**, 389–398 (2023).
41. Gin, S. et al. Insights into the mechanisms controlling the residual corrosion rate of borosilicate glasses. *npj Mater. Degrad.* **4**, 41 (2020).
42. Ping, Z., Nguyen, Q., Chen, S., Zhou, J. & Ding, Y. States of water in different hydrophilic polymers—DSC and FTIR studies. *Polym* **42**, 8461–8467 (2001).

43. Kamitsos, E. I., Karakassides, M. A. & Chryssikos, G. D. Cation network interactions in binary alkali-metal borate glasses - a far-infrared study. *J. Phys. Chem.* **91**, 5807–5813 (1987).
44. Tournie, A. et al. Impact of boron complexation by Tris buffer on the initial dissolution rate of borosilicate glasses. *J. Colloid Interface Sci.* **400**, 161–167 (2013).
45. Kreisberg, V. A., Rakcheev, V. P. & Antropova, T. V. Influence of the acid concentration on the morphology of micropores and mesopores in porous glasses. *Glass Phys. Chem.* **32**, 615–622 (2006).
46. Ziegler, J. F., Ziegler, M. D. & Biersack, J. P. SRIM - The stopping and range of ions in matter (2010). *Nucl. Instrum. Meth B* **268**, 1818–1823 (2010).
47. ASTM International. Standard test method for static leaching of monolithic waste forms for disposal of radioactive waste. https://doi.org/10.1520/C1220-21 (2010).

ACKNOWLEDGEMENTS

This work was supported by the National Natural Science Foundation of China (Grant Nos. 12175092 and U1867207), and Natural Science Foundation of Gansu Province (Grant No. 23JRRA1042) and State Key Laboratory of Nuclear Physics and Technology, Peking University under Grant No. NPT2021KFJ42. Kemian Qin was supported by INWARD coordinated research project [Ion Beam Irradiation for High Level Nuclear Waste Form Development, F11022] from IAEA.

AUTHOR CONTRIBUTIONS

K.Q.: Conceptualization, Methodology, Investigation, Data curation, Formal analysis, Writing—original draft. B.Z.: Investigation, Writing—review & editing. Z.J.: Investigation, Writing—review & editing; Y.W.: Investigation, Writing—review & editing. Y.P.: Writing—review & editing. Y.S.: Investigation. K.B.: Investigation. S.Z.: Investigation. T.W.: Resources, Writing—review & editing. H.P.: Conceptualization, Methodology, Resources, Supervision, Funding acquisition, Writing—review & editing.

COMPETING INTERESTS

The authors declare no competing interests.

ADDITIONAL INFORMATION

Supplementary information The online version contains supplementary material available at https://doi.org/10.1038/s41529-024-00426-0.

Correspondence and requests for materials should be addressed to Haibo Peng.

Reprints and permission information is available at http://www.nature.com/reprints

Publisher's note Springer Nature remains neutral with regard to jurisdictional claims in published maps and institutional affiliations.